

FULL PAPER

Assembly immobilized palladium(0) on carboxymethylcellulose/ Fe_3O_4 hybrid: An efficient tailor-made magnetically catalyst for the Suzuki–Miyaura couplings

Zhuan Zhang | Yizong Zhang | Xiaoping Liu | Binbin Shen | Tianzhu Zhang | Yiqun Li Department of Chemistry, Jinan University,
Guangzhou 510632, China**Correspondence**Yiqun Li, Department of Chemistry, Jinan
University, Guangzhou 510632, China
Email: tlyq@jnu.edu.cn**Funding information**National Natural Science Foundation of
China, Grant/Award Number: 21372099 and
21072077; Natural Science Foundation of
Guangdong Province, Grant/Award Number:
10151063201000051 and
8151063201000016

The Pd nanoparticles (Pd NPs) embedded on magnetically retrievable carboxymethylcellulose/ Fe_3O_4 ($\text{Pd}^0\text{@CMC/Fe}_3\text{O}_4$) organic/inorganic hybrid were prepared via the conventional simple process. The presence of the hydroxyl and carboxyl groups within the framework of the magnetic hybrid enables the facile preparation and stabilization of Pd NPs in this organic/inorganic hybrid. This hybrid catalyst was very effective in the Suzuki–Miyaura reaction of a variety of aryl halides with arylboronic acid to afford excellent product yields. The catalyst showed good stability and could be easily recovered with an external magnetic field and reused for several times without a significant loss in its catalytic activity. Furthermore, the $\text{Pd}^0\text{@CMC/Fe}_3\text{O}_4$ hybrid catalyst was fully characterized by UV–Vis, FT–IR, XRD, SEM, EDX, TEM, XPS and TGA techniques. The hot filtration test suggests that a homogeneous mechanism is operative in Suzuki–Miyaura reaction.

KEYWORDS

carboxymethylcellulose, catalyst, magnetic nanohybrid, palladium nanoparticles, Suzuki–Miyaura reaction

1 | INTRODUCTION

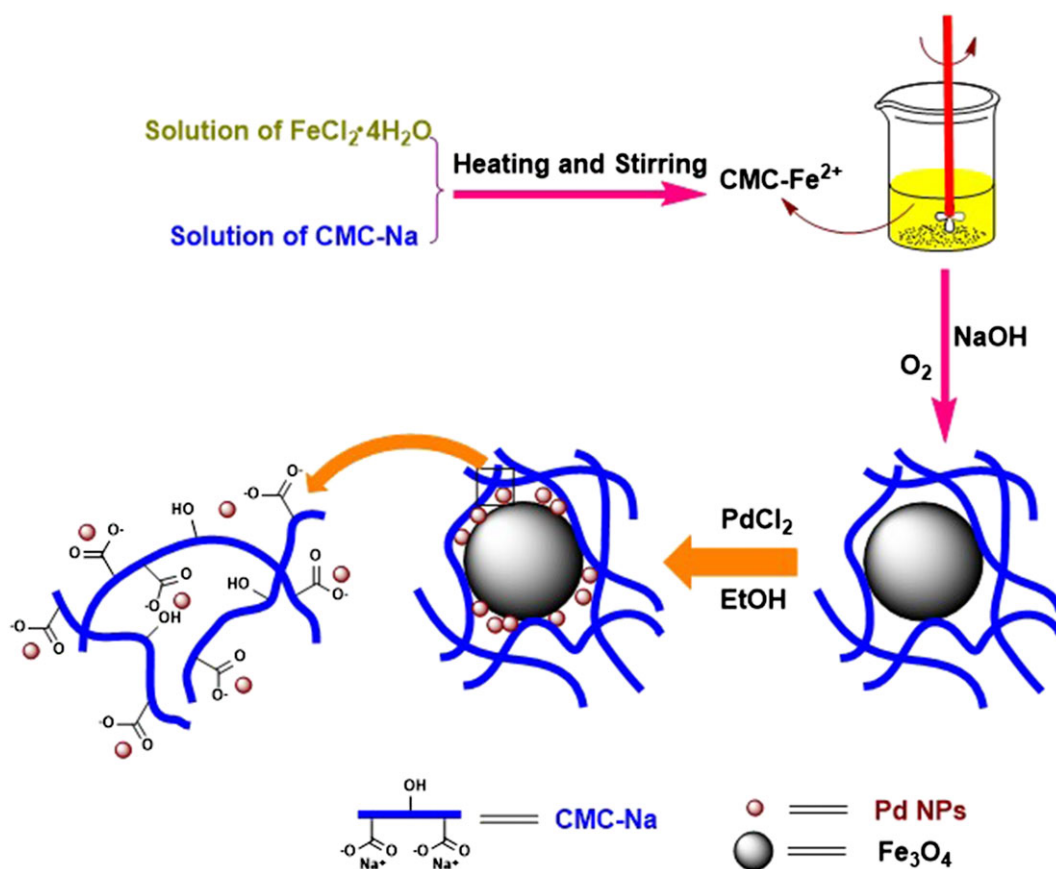
The Suzuki–Miyaura reactions^[1–3] provide an attractive and efficient route to construct $\text{C}_{\text{sp}2}\text{–C}_{\text{sp}2}$ bond for the synthesis of a variety of important chemicals or structural motif for their applications in pharmaceuticals and advanced materials. Traditionally, palladium is one of the most commonly employed catalysts which can be performed under both homogeneous and heterogeneous conditions.^[4] In general, the wide use of homogeneous Pd catalysts is based on Pd(II) complexes^[5,6] such as phosphanes, N–heterocyclic carbenes, oxime carbapalladacycle and imidazolium, and so on. They display high catalytic activity and selectivity, excellent versatility, rapid reaction rates, and large turnover numbers. The major disadvantages of such catalytic systems are the recovery of the catalyst as well as the instability and toxicity of ligands. Moreover, aggregation and precipitation of palladium metal in the homogeneous systems always lead to lost activity of the catalysts. This fact rationalizes that it is

reasonable and feasible to immobilize a catalytic Pd(II) complex on the heterogeneous bed to mitigate these problems. However, the catalytic sites in heterogeneous catalysts are not as accessible as in a homogeneous system, and thus the activity of the catalyst is usually reduced.^[6,7] Consequently, a semi-heterogeneous catalysis^[8] combining the characteristics of heterogeneous catalysis (ease of catalyst separation and recovery) with those of homogeneous catalysis (high activity and selectivity) is the goal that may be achieved by Pd NPs. Pd NPs, which possess several advantages such as excellent activity, greater selectivity, and high stability over conventional catalyst systems, partially due to their large surface-to-volume ratios,^[8–10] are widely used for C–C cross coupling reactions.^[11–13] Unfortunately, Pd NPs are unstable and easily aggregate and precipitate to bulk metal and, therefore, decrease the catalytic activity. Moreover, isolation and recovery of these tiny nanocatalysts from the reaction mixture are tedious. Generally, the aggregation of Pd NPs can be avoided by using suitable stabilizers or

supporting materials.^[14] In fact, stability, reactivity, and reusability of Pd NPs are highly depended on the type of selected materials using immobilized matrix. Some Pd NPs catalysts which are immobilized onto inorganic supports (such as carbon, carbon nanotubes, different metal oxides, silica gel and modified silica gel, hydroxyapatite, molecular sieves, etc.) and organic supports (such as polystyrene, polyaniline, polyvinylpyrrolidone, hydrogel, biopolymer, and so forth) have been reviewed.^[15–17] The design and preparation of novel hybrid catalyst^[18–20] with superior activities and unique potential application in catalysis have attracted extensive attention in the academic and industrial community in recent years. Although there has been some tremendous progress in this area in recent years, a number of problems still remain to be addressed. One of the biggest challenges is catalyst recovering and reuse when the size of support is decreased to the nanometer scale. The separation of nanocatalysts from the reaction mixture is almost impossible merely dependent on the use of the filter, high-speed centrifugation, or precipitation. This is the major reason why magnetic nanoparticles (MNPs) are used as viable alternatives to conventional supporting materials for immobilization of catalyst. The unique paramagnetic character of MNPs is that the catalyst based on them can be easily recovered from the reaction mixture simply by using an external magnet, thus eliminating the

necessity of traditional separation steps. Another big challenge is to develop efficiently immobilized systems that could simultaneously fulfill the demand of achieving high catalytic activity.

Fe₃O₄ MNPs have emerged as smart materials for heterogeneous catalyst due to their intrinsic properties such as paramagnetic character, high surface area, good chemo-stability, and low toxicity and biocompatible. Bare Fe₃O₄ MNPs materials can be directly used for immobilization of Pd nanoparticles,^[21–23] but in most cases, leaching of active species is unavoidable for this material, so the reactivity of catalyst is decreased. The surface of Fe₃O₄ MNPs can be post-functionalized by organic moieties using a chemical process to improve its applicability as support in preparation of Pd NPs catalysts. Recently, more effort has been focused on the surface post-modification of MNPs with suitable ligands to anchor the catalytic active species.^[24] However, this protocol has some defects such as multistep synthetic processes using expensive reagents and solvents, and relatively low loading of catalysts. In order to overcome these drawbacks, magnetic organic/inorganic hybrid materials may be an effective alternative for the post-functionalization of Fe₃O₄. One of the most abundant polyhydroxyl materials, which have been widely employed for immobilization and stabilization of Pd NPs *via* the chelation with transition metals and



SCHEME 1 Schematic pathway for the preparation of the magnetic palladium hybrid catalyst

hydroxyl groups or carboxyl groups^[25] is natural hydroxyl biopolymer and its derivatives such as cellulose, carboxymethylcellulose, chitosan, starch. When ligated moieties such as polyhydroxyl or carboxyl groups are hybridized with Fe₃O₄ MNPs, most of these problems can be settled. In light of this, we have reported highly efficient catalysts for Suzuki–Miyaura couplings based on immobilization of Pd NPs on cellulose or carboxymethylcellulose in our previous work. Sodium carboxymethylcellulose (CMC–Na) carrying a tremendous number of carboxymethyl groups (–CH₂–COO[–]Na⁺) has excellent cation exchange capacity.^[26,27] Considering this characteristic, CMC–Na has been reported to serve as a template for the preparation of magnetic Fe₃O₄ organic/inorganic hybrid.

2 | RESULTS AND DISCUSSION

2.1 | Preparation and characterization of Pd⁰@CMC/Fe₃O₄ catalysts

The magnetic nanocatalyst consisting of Pd NPs on a CMC/Fe₃O₄ hybrid was prepared in two easy steps. In the first step, the Na–CMC/Fe₃O₄ NPs hybrid was prepared *via* two-step metathesis and one-step oxidation procedures according to our previous work.^[28] In the second step, the as-prepared Na–CMC/Fe₃O₄ hybrid was treated with Pd (II) aqueous solution for overnight based on the property of CMC–Na being capable of exchanging with Pd(II). The obtained Pd^{II}@CMC/Fe₃O₄ hybrid catalyst was filtered off and washed thoroughly with water and excessive ethanol. The Pd⁰@CMC/Fe₃O₄ organic/inorganic hybrid catalyst thus obtained *via* the reduction of Pd²⁺ ions with EtOH to form the Pd(0) element, which assembled and nucleated on the CMC/Fe₃O₄ hybrid supports. Scheme 1 displays the schematic illustration of the formation of the Pd⁰@CMC/Fe₃O₄ NPs hybrid consisting of superparamagnetic Fe₃O₄ nanoparticles, CMC and Pd(0) species.

Then, the as-prepared hybrid catalyst was fully characterized by FT-IR, ICP-AES, XRD, SEM, EDX, TEM, and TGA techniques.

Figure 1 shows the FT-IR spectra for CMC–Na, Na–CMC/Fe₃O₄, and Pd⁰@CMC/Fe₃O₄ hybrid. A strong and broad absorption band at 3000–3750 cm^{–1} is related to the –OH group stretching vibrations. In curve b and c, the strong vibration of Fe–O bonds at 580 cm^{–1} or 588 cm^{–1} indicate the presence of Fe₃O₄.^[29] In curve a, the characteristic peaks at 1615 cm^{–1} and 1423 cm^{–1} are assigned to the carboxylate (–COO[–]Na⁺) asymmetric and symmetric stretching vibration.^[30,31] The absorption peaks at 1593 cm^{–1} and 1410 cm^{–1} shifted to lower wavenumbers in curve b confirms the hybridization of CMC and Fe₃O₄. Furthermore, these carboxylate characteristic peaks in curve c shift to 1628 cm^{–1}

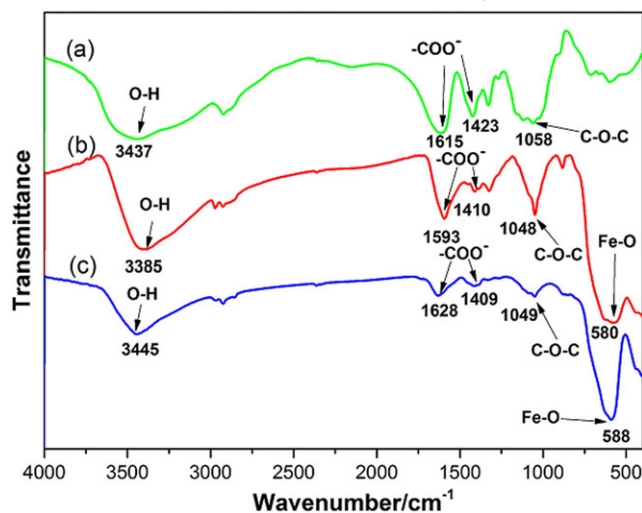


FIGURE 1 FT-IR spectra of CMC–Na (a), Na–CMC/Fe₃O₄ (b), and Pd⁰@CMC/Fe₃O₄ (c)

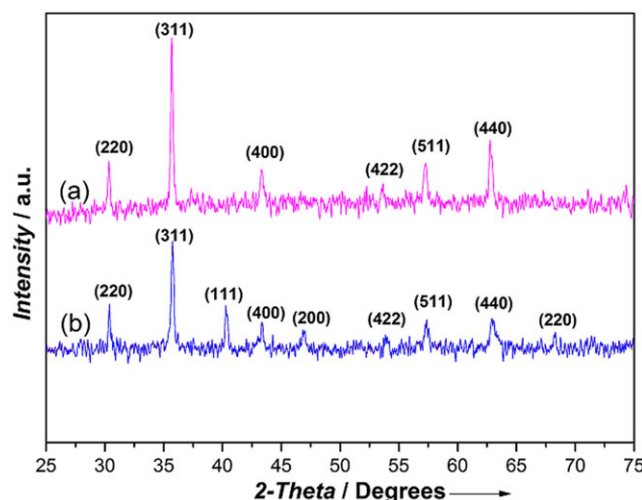


FIGURE 2 XRD patterns of bare Fe₃O₄ (a), Pd⁰@CMC/Fe₃O₄ (b)

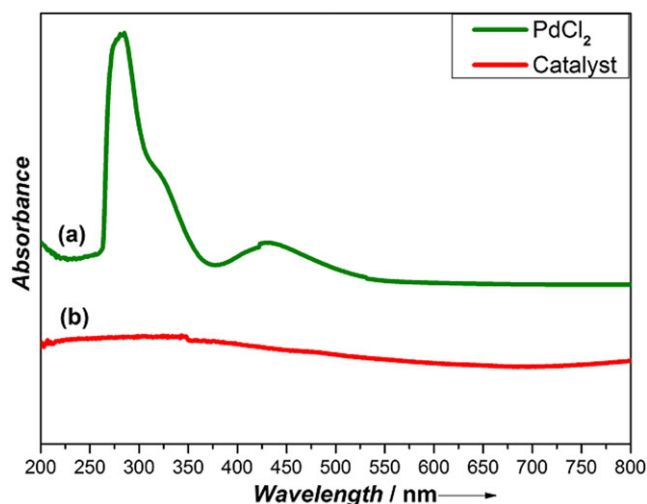


FIGURE 3 UV/Vis spectra of PdCl₂ (a), Pd⁰@CMC/Fe₃O₄ (b)

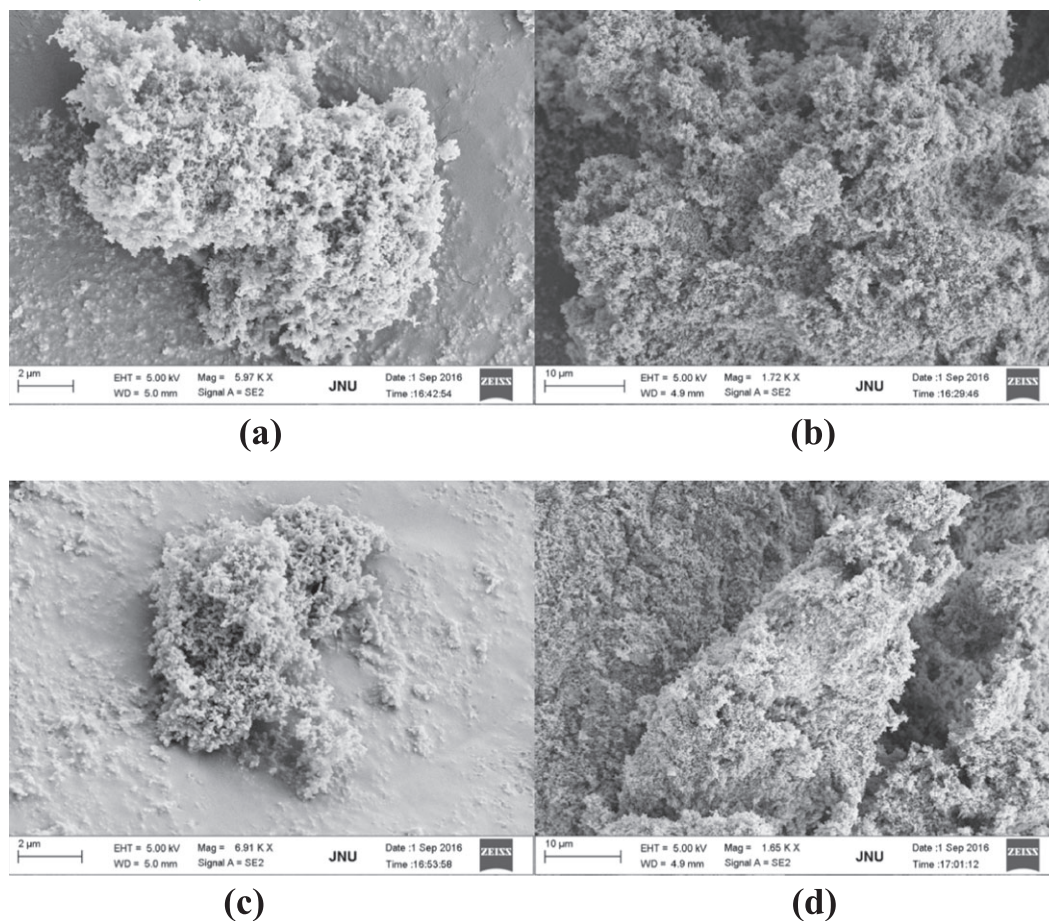


FIGURE 4 FESEM images of fresh catalyst (a), (b) and recovered catalyst (c), (d) at the same magnifications

and 1409 cm^{-1} , which indicated the coordination of palladium with carboxylate groups.

The crystallinity of the resulting products was investigated by X-ray diffraction (XRD). Figure 2 shows the XRD pattern of the $\text{Pd}^0\text{@CMC/Fe}_3\text{O}_4$. The diffraction peaks at 2θ of 30.1° , 35.4° , 43.1° , 53.4° , 57° , and 62.6° are assigned to the diffraction of (220), (311), (400), (422), (511) and (440) of the Fe_3O_4 (JCPDS 89–3854).^[29] All diffraction

peaks are in perfect agreement with the standard structure of Fe_3O_4 nanoparticles (curve a). The peaks at 2θ of 40.1° , 46.7° and 68.1° correspond to the diffraction of (111), (200) and (220) of the Pd nanoparticles.^[29] The XRD pattern suggests that Pd^0 is successfully immobilized on the hybrid.

The UV–Vis spectrum of $\text{Pd}^0\text{@CMC/Fe}_3\text{O}_4$ hybrid was also studied. According to the literature results, the UV–Vis spectrum of PdCl_2 revealing a peak at 280 nm refers to the

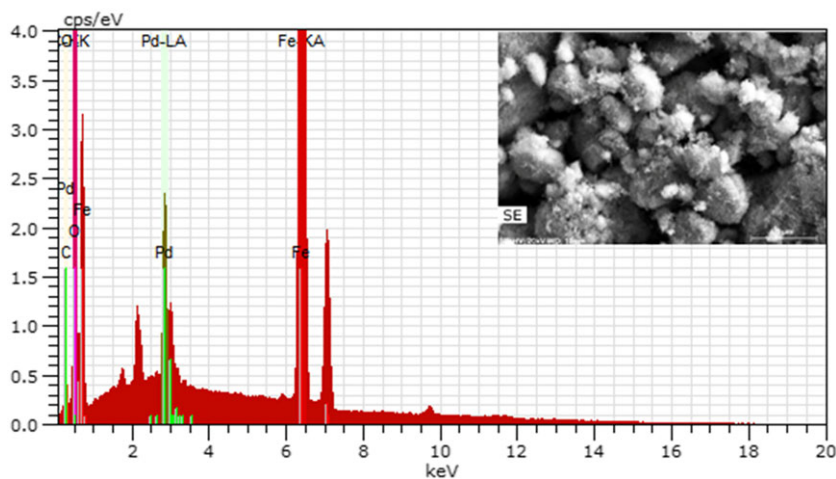


FIGURE 5 EDS data for the fresh catalyst

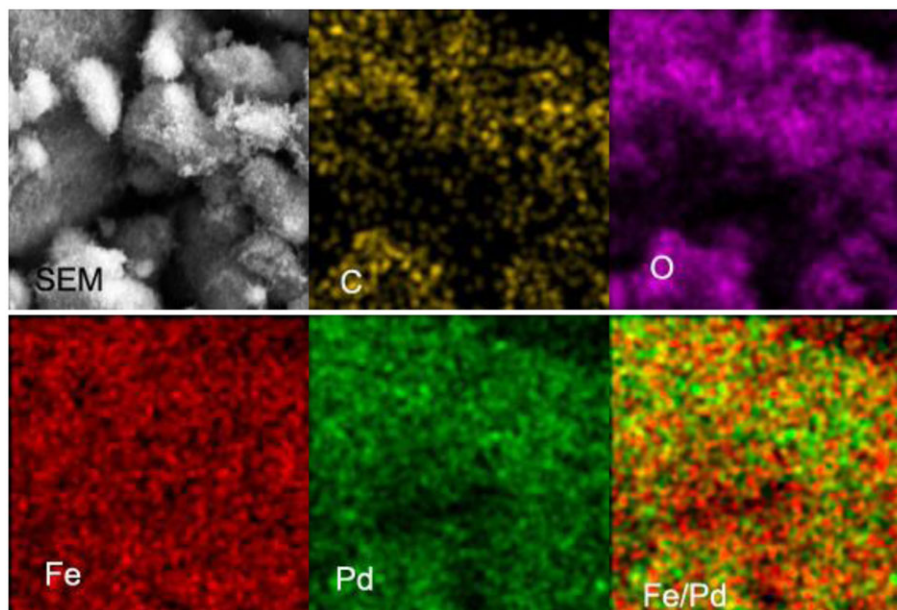


FIGURE 6 SEM images of Pd⁰@CMC/Fe₃O₄ shows the presence of C, O, Fe, Pd atoms in the catalyst

existence of Pd(II) (Figure 3a).^[32] However, there was not any obvious peak at 280 nm in the UV–Vis spectrum of Pd⁰@CMC/Fe₃O₄ hybrid, which indicated a major reduction of Pd(II) to Pd nanoparticles in the catalyst.

The morphology of the fresh catalyst and reused catalyst was characterized by Field Emission Scanning Electron Microscope (FE-SEM). FE-SEM images in Figure 4 are presented at two different magnifications (10 μm and 2 μm). FE-

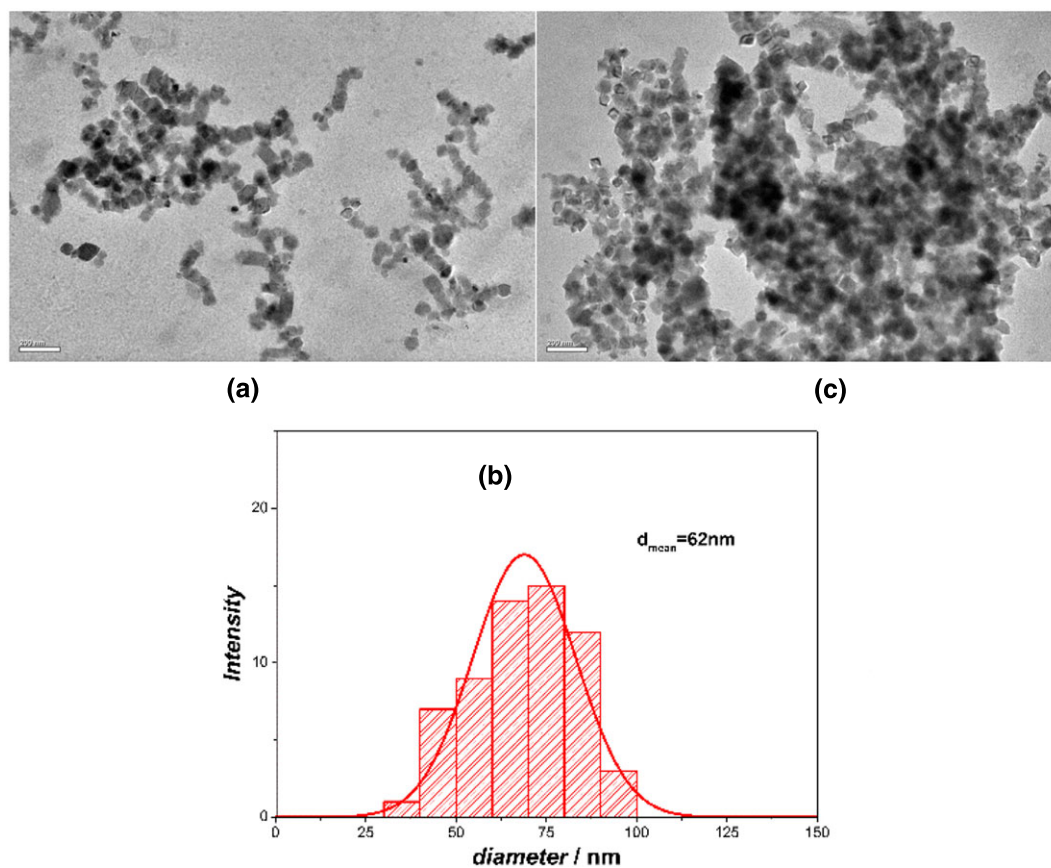


FIGURE 7 TEM images of fresh catalyst (a), nanoparticle diameter histogram (b), and recovered catalyst (c)

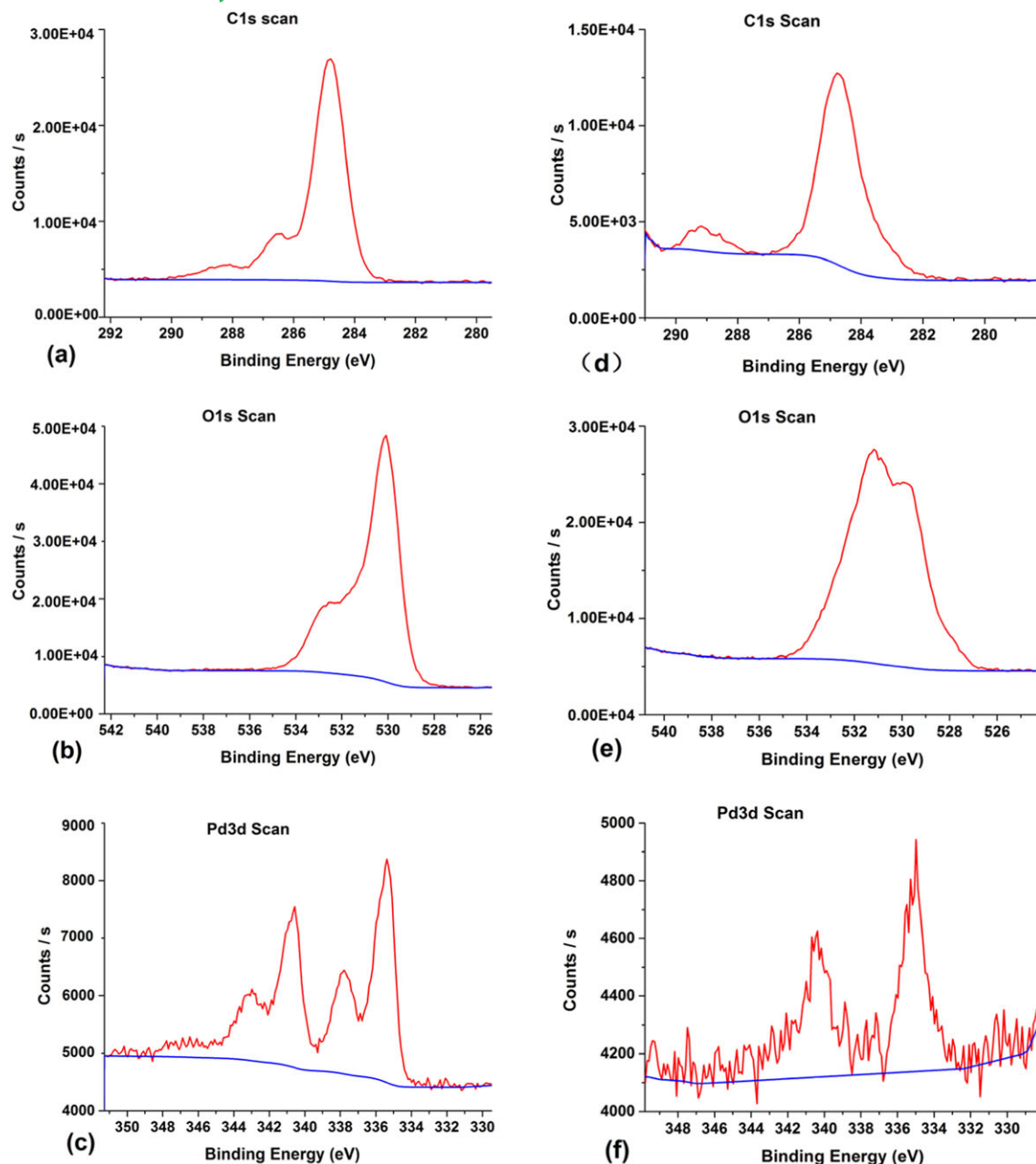


FIGURE 8 XPS images of fresh catalyst (images of a, b, c) and recovered catalyst (images of d, e, f)

SEM images clearly show a flocculated morphology with porous nature, which facilitates the better mass transfer and enlarges its contact area. Hence porous support increases catalytic activity and also avoids Pd leaching. Furthermore, the morphology of recovered catalyst remained intact after three recoveries.

The presence of Pd species in the catalyst can be also confirmed by energy-dispersive X-ray spectroscopy (EDS) coupled with SEM analysis (Figure 5). The EDS of fresh catalyst clearly indicates the presence of C, O, Fe and Pd in the organic/inorganic hybrid. Obviously, the presence of these elements implies the existing of Pd, CMC, and Fe_3O_4 in the hybrid catalyst.

Figure 6 shows a representative FE-SEM image and corresponding elemental maps for the synthesized catalyst. It clearly exhibited that metallic Pd nanoparticles are well dispersed in the catalyst. At the same time, the selected-area elemental analysis indicates the existence of C, O, Fe and Pd throughout hybrid in a homogeneous manner.

In order to get insight into the morphology of the hybrid, the field emission transmission electron microscopy (FE-TEM) images of the fresh and used $\text{Pd}^0/\text{CMC}/\text{Fe}_3\text{O}_4$ were recorded (Figure 7) showing the formation of quasi-spherical nanoparticles (Figure 7a). The size distribution plot (Figure 7b) obtained from TEM measurements show the average particle size is located around 62 nm. (Figure 7b). Furthermore,

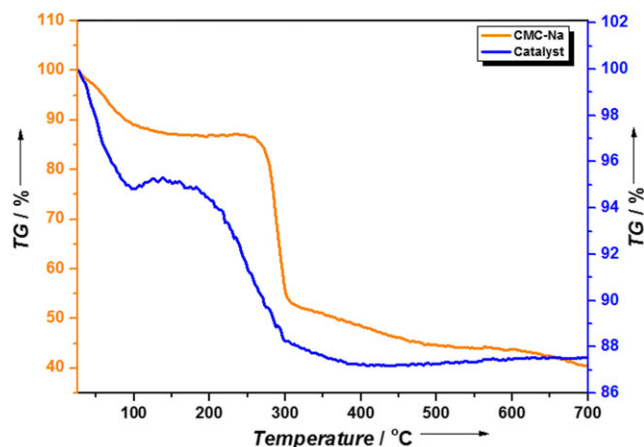


FIGURE 9 TGA diagram of catalyst and CMC–Na

the preserve of the morphology and the size of the reused catalyst after the third run are observed (Figure 7c) by comparison with the fresh catalyst.

XPS was used to investigate the valence state of the fresh catalyst and reused catalyst. As shown in Figure 8, it can be seen that the binding energies of C_{1s} in the fresh catalyst are the same as the reused catalyst around

284.78 eV, which indicates the existence of CMC. The binding energies of O_{1s} in the fresh catalyst and reused catalyst are about 530.08 eV and 531.18 eV respectively, which proves the interaction between Pd NPs and CMC. It could also be found that the existence of two intense doublets at 335.38 and 340.58 eV related to Pd(0) and peaks at 337.78 and 342.98 eV related to Pd(II) corresponding to Pd $3d_{5/2}$ and Pd $3d_{3/2}$ in the fresh catalyst respectively, which indicates that about 64% of palladium particles exist in the form of Pd(0). Nevertheless, only strong peaks at 335.28 eV and 340.68 eV corresponding to Pd $3d_{5/2}$ and Pd $3d_{3/2}$ can be seen in the reused catalyst, which shows the main existence of Pd NPs after the reaction.^[33,34]

Thermogravimetric analysis (TGA) was used to evaluate the thermal stability of the catalyst, which was conducted in nitrogen atmosphere varying from 25 to 700 °C. As can be seen from the TGA plot in Figure 9, there are two-step thermal decomposition. The first weight loss occurred around 100 °C is attributed to the removal of loosely physically adsorbed water. Then the main weight loss began near 200 °C due to the decomposition of CMC. By comparison with the TGA of CMC–Na, the stability of Pd⁰@CMC/Fe₃O₄ is less than that of CMC–Na.

TABLE 1 Optimization of the Suzuki-Miyaura Reactions Condition^a

Entry	Solvent (v/v)	Base	Catalyst (mol%)	Temp (°C)	Time [min]	Yield [%]
1	EtOH/H ₂ O (75/25)	K ₂ CO ₃	0.9	78	15	92
2	EtOH	K ₂ CO ₃	0.9	78	20	87
3	MeOH	K ₂ CO ₃	0.9	78	30	78
4	DMF	K ₂ CO ₃	0.9	78	30	77
5	H ₂ O	K ₂ CO ₃	0.9	78	30	65
6	CH ₃ CN	K ₂ CO ₃	0.9	78	30	70
7	DMSO	K ₂ CO ₃	0.9	78	30	76
8	EtOH/H ₂ O (75/25)	Na ₂ CO ₃	0.9	78	50	75
9	EtOH/H ₂ O (75/25)	Na ₃ PO ₄ ·12H ₂ O	0.9	78	30	84
10	EtOH/H ₂ O (75/25)	CS ₂ CO ₃	0.9	78	20	82
11	EtOH/H ₂ O (75/25)	K ₃ PO ₄ ·3H ₂ O	0.9	78	20	84
12	EtOH/H ₂ O (75/25)	CH ₃ ONa	0.9	78	30	80
13	EtOH/H ₂ O (75/25)	NaOH	0.9	78	30	80
14	EtOH/H ₂ O (75/25)	K ₂ CO ₃	0.3	78	30	79
15	EtOH/H ₂ O (75/25)	K ₂ CO ₃	0.6	78	15	90
16	EtOH/H ₂ O (75/25)	K ₂ CO ₃	1.2	78	15	92
17	EtOH/H ₂ O (75/25)	K ₂ CO ₃	1.5	78	15	91
18	EtOH/H ₂ O (75/25)	K ₂ CO ₃	0.9	60	30	80
19	EtOH/H ₂ O (75/25)	K ₂ CO ₃	0.9	40	120	60
20	EtOH/H ₂ O (75/25)	K ₂ CO ₃	0.9	rt	480	45

^aReaction conditions: aryl halide (1 mmol), phenylboronic acid (1.2 mmol), base (2 mmol), catalyst (0.9 mol% of Pd), solvent (5 mL) at specific temperature.

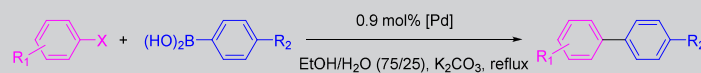
2.2 | Catalytic performance of Pd⁰@CMC/ Fe₃O₄ hybrid in Suzuki–Miyaura reaction

To evaluate the effect of base, catalyst loading, solvent, and temperature, the cross-coupling of *p*-iodoanisole and phenyl boronic acid was conducted as a model reaction.

Initially, the influence of different bases was investigated on the model reaction in the aqueous ethanol (EtOH/H₂O, *v/v* = 75/25) at reflux. Among the explored bases, K₂CO₃ was found to be the top one to afford the highest yields of 92%, respectively (Table 1, entry 1). Solvents play a crucial role in the Suzuki–Miyaura coupling reaction. Screening of solvents indicated that the mixed solvent of EtOH/H₂O (*v/v* = 75/25) is the best choice for this catalytic system, which makes this reaction quite efficient.

The effects of the catalyst amount are also investigated. As can be seen from Table 1, the yield of the cross-coupling product increased with the increase of catalyst. The highest yield of 92% was obtained in the presence of 0.9 mol% of Pd (Table 1, entry 1). It is observed that increasing the amount of catalyst from 0.9 to 1.2, even to 1.5 mol%, the yield of desired product does not change significantly. Besides, upon decreasing quantity of catalyst from 0.9 to 0.6, and even to 0.3 mol%, the yield of the product decreases from 92 to 90, and 79% in prolonging reaction time, respectively. The effect of reaction temperature on the model reaction was also explored. It is clearly showed that the yields of the product significantly decreased with the decrease of temperature. We have concluded that the best result was obtained when the model

TABLE 2 The Suzuki–Miyaura Coupling of Aryl Halide with Arylboronic Acid^a



Entry	R ₁	R ₂	X	Time [h]	Yield [%]	Product
1	4-MeO	H	I	0.25	92	a
2	4-MeO	4-MeO	I	0.25	93	b
3	4-MeO	4-Me	I	0.25	90	c
4	4-MeO	4-F	I	0.25	92	d
5	4-MeO	4-CHO	I	0.25	91	e
6	4-Me	H	I	0.50	83	f
7	4-NO ₂	H	I	0.25	95	g
8	4-NO ₂	4-MeO	I	0.25	96	h
9	4-NO ₂	4-Me	I	0.25	85	i
10	4-NO ₂	4-F	I	0.25	96	j
11	4-NO ₂	4-CHO	I	0.25	92	k
12	H	H	I	0.5	80	l
13	H	4-MeO	I	0.5	92	a
14	H	4-Me	I	0.5	85	f
15	H	4-F	I	0.5	87	m
16	H	4-CHO	I	0.5	85	n
17	3-NO ₂	H	I	0.5	94	o
18	3-NO ₂	4-MeO	I	0.25	96	p
19	4-NH ₂	H	I	0.5	90	q
20	4-NH ₂	4-MeO	I	0.5	92	r
21	4-NO ₂	H	Br	1.0	93	g
22	4-NO ₂	4-MeO	Br	1.0	92	h
23	4-NO ₂	4-Me	Br	1.0	90	i
24	4-NO ₂	4-F	Br	1.0	92	j
25	4-NO ₂	4-CHO	Br	1.0	89	k
26	4-MeO	H	Br	1.0	88	a
27	4-MeO	4-MeO	Br	1.0	90	b
28	4-Me	4-MeO	Br	1.0	80	c

^aReaction conditions: aryl halide (1 mmol), phenylboronic acid (1.2 mmol), K₂CO₃ (2 mmol), catalyst (0.9 mol % of Pd), EtOH/H₂O (*v/v* = 75/25, 5 mL) at 78 °C.

^bIsolated yields

reaction was carried out with 0.9 mol % of the catalyst using K_2CO_3 as a base in the aqueous ethanol (EtOH/ H_2O , $v/v = 75/25$) at reflux.

To explore the scope and generality of the catalyst, the optimized protocol was applied for reactions of a variety of substituted aryl halides with arylboronic acids. The results are presented in Table 2. In all cases, both activated and deactivated aryl iodides and aryl bromides were completely converted into the corresponding biaryls in 80–96% yields within 15 min–1 h. Aryl iodides possessing either electron-withdrawing or electron-donating group produced the corresponding biaryls in good yields, whereas aryl bromide required prolonging time in order to obtain excellent yields. Notably, the electronic effects (electron donating or electron withdrawing) of the substituents of the arylboronic acids had a negligible influence on reactivity.

2.3 | Recyclability of the catalyst and characterization of the used catalyst

One crucial for practical application of magnetic catalyst is convenient recovery, reusability, stability, and leaching. For this propose, the reusability of the catalyst was investigated using the model reaction. The catalyst was separated by external magnet after each run (Figure 10), washed adequately with ethyl acetate, dried, and applied in subsequent runs. It is found that the catalyst can be reused at least six consecutive runs without significant loss of its activity (Figure 11). This catalyst demonstrated great thermal stability with high activity at reflux temperatures. The FE-SEM (Figure 4b) image of the used catalyst after the reaction under thermal conditions indicated that the surface morphology of the magnetic hybrid nanocatalyst was not changed. The FE-TEM (Figure 7c) image showed the morphology and size of the catalyst after

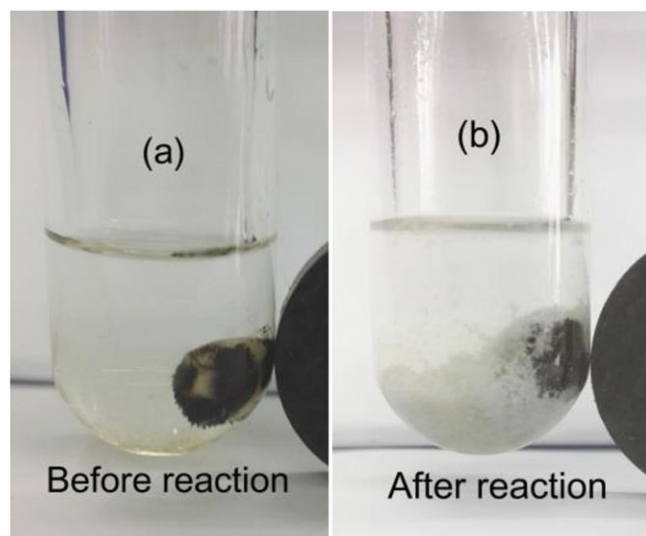


FIGURE 10 $Pd^0@CMC/Fe_3O_4$ dispersed in the reaction mixture (a), the magnetic isolation of the catalyst by a magnet (b)

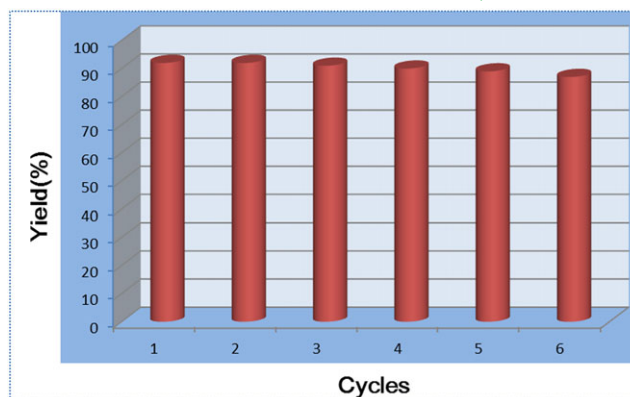


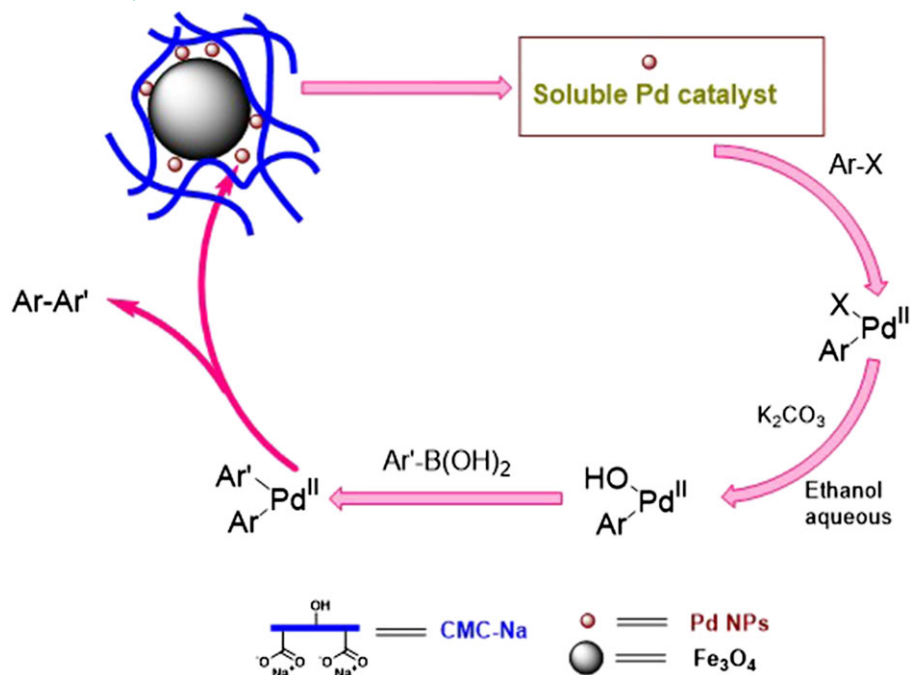
FIGURE 11 Recycling and reuse of $Pd^0@CMC/Fe_3O_4$ in the Suzuki-Miyaura reaction

three runs with slightly agglomerate, which implies the soluble and active $Pd(0)$ species redeposited onto the catalyst to form slight larger $Pd(0)$ nanoparticles at the end of the catalytic reaction.

2.4 | Homogenous mechanism for Suzuki–Miyaura reaction

To determine the homogeneous/heterogeneous nature of the catalytic system, we have also performed the hot filtration test^[6] using model reaction. During this test, the catalyst was removed from the reaction mixture by external magnet after 5 min, and the reaction was then allowed to further react till the completion in 83% product yield, indicating that catalytically active Pd species remained in the filtrate. To further confirm the homogeneity of the catalytic system, potential Pd leaching into the reaction mixture was also measured with ICP-AES analysis. The analysis result showed that the Pd concentration in the reaction solution after one run was 9.4×10^{-4} mmol/l, which corresponds to around 0.20% of the starting Pd -amount. Both findings suggest that the catalyst is characteristic homogeneous in nature, and the soluble $Pd(0)$ species or soluble $Pd(0)$ nanoparticle clusters are the true catalytic species.

Based on the above-mentioned hot filtrate test, ICP analysis, and the previous reports, we propose a tentative pathway for this transformation (Scheme 2). The mechanism by which this occurs involves the generation of a soluble, catalytically active $Pd(0)$ species that is released from and redeposited onto the catalyst to form slight larger $Pd(0)$ nanoparticles after the reaction (Figure 7). The first step is an oxidative addition, which the leaching active $Pd(0)$ species inserts into the aryl halide bond. The last step in all coupling reactions is the regeneration and redeposition of $Pd(0)$ species on the surface of the magnetic hybrid by reductive elimination of the $Pd(II)$ compound in the presence of a base.^[35]



SCHEME 2 Plausible mechanism for the Suzuki-Miyaura coupling

3 | CONCLUSION

In summary, a novel magnetic organic/inorganic hybrid materials (CMC/Fe₃O₄) supported Pd nanoparticles (Pd⁰@CMC/Fe₃O₄) was prepared by a simple and low-cost approach without using any expensive organosilane. The as-synthesized Pd⁰@CMC/Fe₃O₄ hybrid exhibited excellent catalytic activities for Suzuki–Miyaura cross-coupling reactions in excellent yields under aerobic conditions. The high catalytic activity of the catalyst can be attributed to the coordination with both carboxyl groups and free hydroxyl groups within the magnetic CMC/Fe₃O₄ hybrid, which prevents the agglomeration of Pd NPs. The magnetic hybrid catalyst was easily separated by application of an external magnetic field and could be recycled at least six times without significant loss of its reactivity, which makes it an attractive catalytic system for the coupling reaction under mild condition. Therefore, it is believed that this synthetic protocol described here would greatly contribute to an environmentally greener and safer process.

4 | EXPERIMENTAL

4.1 | Chemicals and characterization

Sodium carboxymethylcellulose (CMC–Na, Mw 250,000) and other chemicals were purchased from commercial sources and used as received without further purification. Na–CMC/Fe₃O₄ hybrid was prepared with a slight modification according to our previous work.^[28]

Melting points were measured by an Electrothermal X6 microscopic digital melting point apparatus. Fourier transform infrared spectra (FT-IR) were recorded on a Nicolet 6700 FT-IR spectrometer using KBr pellet. X-Ray Powder Diffraction (XRD) data were collected on an MSALXRD2 diffractometer using Cu *K* α radiation in a range of Bragg's angles (10–80°). Scanning electron microscopy (SEM) was conducted with a Philips XL 30ESEM instrument. Transmission electron microscopy (TEM) was obtained with a Philips Tecnai instrument. Thermogravimetric analysis (TGA) was operated on a Netzsch STA449F3 in the range of 25–700 °C under nitrogen atmosphere. ¹H NMR spectra were recorded on a Bruker-300 Avance Spectrometer with CDCl₃ as solvent and TMS as internal standard. The elemental Pd content of the catalyst was determined by inductively coupled plasma-atomic emission spectrometry (ICP-AES) using Perkin Elmer Optima 2000 DV.

4.2 | Preparation of Pd⁰@CMC/Fe₃O₄ magnetic catalyst

PdCl₂ aqueous solution (0.60 mmol PdCl₂) was added into 100 ml aqueous solution dispersed Na–CMC/Fe₃O₄ (1 g) with constantly stirring at room temperature for 24 h. The resulting solid was separated from the mixture with external magnetic field and washed successively with deionized water and anhydrous ethanol thoroughly, then dried in vacuum to constant weight to provide Pd⁰@CMC/Fe₃O₄ as a powder. The Pd content was determined to be 0.46 mmol/g by ICP-AES.

4.3 | General procedure for the catalytic Suzuki–Miyaura reaction

The aryl halide (1 mmol), arylboronic acid (1.2 mmol), K_2CO_3 (2 mmol), and a catalytic amount of $Pd^0@CMC/Fe_3O_4$ catalyst (0.9 mol% of Pd) were added to 5.0 ml aqueous ethanol (EtOH/ H_2O , $v/v = 75/25$). The reaction mixture was stirred under reflux condition for a specific time. The progress was tracked by TLC. After completion of the reaction, ethyl acetate was added to the flask and the magnetic catalyst was collected by an external magnet, washed with ethyl acetate thoroughly, and dried in air for the next run. The organic phase was washed with brine and dried over anhydrous Na_2SO_4 . The product was obtained after removal of the organic solution using a rotary evaporator. The desired pure products were further purified by recrystallization with ethanol/ H_2O mixed solvent. All the products are known and 1H NMR data were found to be identical to those reported in the literature.

ACKNOWLEDGEMENTS

We are grateful to the National Natural Science Foundation of China (Nos. 21372099 and 21072077), Natural Science Foundation of Guangdong Province (Nos. 10151063201000051 and 8151063201000016) for financial support.

REFERENCES

- [1] N. Miyaura, K. Yamada, A. Suzuki, *Tetrahedron Lett.* **1979**, *20*, 3437.
- [2] N. Miyaura, A. Suzuki, *Chem. Rev.* **1995**, *95*, 2457.
- [3] I. Maluenda, O. Navarro, *Molecules* **2015**, *20*, 7528.
- [4] I. Hussain, J. Capricho, M. A. Yawer, *Adv. Synth. Catal.* **2016**, *21*, 3320.
- [5] H. Li, C. C. C. Johansson Seechurn, T. J. Colacot, *ACS Catal.* **2012**, *2*, 1147.
- [6] N. T. S. Phan, M. Van Der Sluys, C. W. Jones, *Adv. Synth. Catal.* **2006**, *348*, 609.
- [7] A. Kumar, G. K. Rao, S. Kumar, A. K. Singh, *Organometallics* **2014**, *33*, 2921.
- [8] D. Astruc, F. Lu, J. R. Aranzaes, *Angew. Chem. Int. Ed.* **2005**, *44*, 7852.
- [9] C. Burda, X. Chen, R. Narayanan, M. A. El-Sayed, *Chem. Rev.* **2005**, *105*, 1025.
- [10] L. D. Pachón, G. Rothenberg, *Appl. Organometal. Chem.* **2008**, *22*, 288.
- [11] T. Noël, S. L. Buchwald, *Chem. Soc. Rev.* **2011**, *40*, 5010.
- [12] M. Pérez-Lorenzo, *J. Phys. Chem. Lett.* **2012**, *3*, 167.
- [13] A. Bej, K. Ghosh, A. Sarkar, D. W. Knight, *RSC Adv.* **2016**, *6*, 11446.

- [14] L. Yin, J. Liebscher, *Chem. Rev.* **2007**, *107*, 133.
- [15] S. Paul, M. M. Islam, S. M. Islam, *RSC Adv.* **2015**, *5*, 42193.
- [16] S. K. Beaumont, *J. Chem. Technol. Biot.* **2012**, *87*, 595.
- [17] P. Taladriz-Blanco, P. Hervés, J. Pérez-Juste, *Top. Catal.* **2013**, *56*, 1154.
- [18] A. Zamboulis, N. Moitra, J. J. E. Moreau, X. Cattoën, M. Wong Chi Man, *J. Mater. Chem.* **2010**, *20*, 9322.
- [19] A. Wight, M. Davis, *Chem. Rev.* **2002**, *102*, 3589.
- [20] A. M. P. Salvo, F. Giacalone, M. Gruttadauria, *Molecules* **2016**, *21*, 1288/1.
- [21] B. Karimi, F. Mansouri, H. M. Mirzaei, *ChemCatChem* **2015**, *7*, 1736.
- [22] L. M. Rossi, N. J. S. Costa, F. P. Silva, R. Wojcieszak, *Green Chem.* **2014**, *16*, 2906.
- [23] A. Derible, C. Diebold, J. Dentzer, R. Gadiou, J.-M. Becht, C. Le Drian, *Eur. J. Org. Chem.* **2014**, 7699.
- [24] H. Woo, K. H. Park, *Catal. Today* **2016**, *278*, 209.
- [25] F. Chen, M. Huang, Y. Li, *Ind. Eng. Chem. Res.* **2014**, *53*, 8339.
- [26] J. Xiao, Z. Lu, Y. Li, *Ind. Eng. Chem. Res.* **2015**, *54*, 790.
- [27] B. R. Vaddula, A. Saha, R. S. Varma, J. Leazer, *Eur. J. Org. Chem.* **2012**, 6707.
- [28] Z. Zhang, P. Song, J. Zhou, Y. Chen, B. Lin, Y. Li, *Ind. Eng. Chem. Res.* **2016**, *55*, 12301.
- [29] Q. Du, W. Zhang, H. Ma, J. Zheng, B. Zhou, Y. Li, *Tetrahedron* **2012**, *68*, 3577.
- [30] F. He, D. Zhao, J. Liu, C. B. Roberts, *Ind. Eng. Chem. Res.* **2007**, *46*, 29.
- [31] J. Liu, F. He, E. Durham, D. Zhao, C. B. Roberts, *Langmuir* **2008**, *24*, 328.
- [32] H. Firouzabadi, N. Iranpoor, A. Ghaderi, M. Gholinejad, S. Rahimi, S. Jokar, *RSC Adv.* **2014**, *4*, 27674.
- [33] M. Gholinejad, M. Seyedhamzeh, M. Razeghi, C. Najera, M. Kompany-Zareh, *ChemCatChem* **2016**, *8*, 441.
- [34] M. Zhu, Y. Wang, C. Wang, W. Li, G. Diao, *Catal. Sci. Technol.* **2013**, *3*, 952.
- [35] S. Byun, J. Chung, J. Kwon, B. Moon Kim, *Chem. – Asian J.* **2015**, *10*, 982.

SUPPORTING INFORMATION

Additional Supporting Information may be found online in the supporting information tab for this article.

How to cite this article: Zhang Z, Zhang Y, Liu X, Shen B, Zhang T, Li Y. Assembly immobilized palladium(0) on carboxymethylcellulose/ Fe_3O_4 hybrid: An efficient tailor-made magnetically catalyst for the Suzuki–Miyaura couplings. *Appl Organometal Chem.* 2017;e3912. <https://doi.org/10.1002/aoc.3912>